Rock Property and Depth Mapping from magnetic data applied to greenfields exploration targeting in the Cloncurry District

David Pratt
Tensor Research
Wollstonecraft, NSW 2065
david.pratt@tensor-research.com.au

James Austin
Mineral Resources CSIRO
Lindfield, NSW 2070
james.austin@csiro.au

Clive Foss
Mineral Resources CSIRO
Lindfield, NSW 2070
clive.foss@csiro.au

SUMMARY

A new method for building a model of the rock property distribution on an unconformity surface (Pratt et al., 2019) presents new opportunities for greenfield exploration in complex geological environments. The method uses the inherent 3D information present in the magnetic tensor to create a model segment on the unconformity surface for every magnetic anomaly on every line in the aeromagnetic survey. Because the tensor is a 3D spatial derivative of the magnetic field, it automatically reduces the influence of regional magnetic field changes to focus the inversion process on the unconformity surface. An expert AI system builds a coherent 3D geological model from the individual model segments, which it then uses to constrain the joint inversion of the tensor data.

We explore the ways in which the maps and rock properties can be used to enhance greenfields exploration by applying the technique to the Cloncurry region of the Mount Isa Inlier. We evaluate the effectiveness of using the compact magnetic rock property estimates to define targets that might otherwise have been missed in the early phase of exploration. Historical airborne data acquired prior to mining of most deposits helps us to design appropriate strategies for targeting similar prospect styles.

Key words: magnetisation, depth, IOCG, skarn, AI.

INTRODUCTION

Transformation of total field magnetic data to the magnetic tensor (Pratt et al., 2020) provides the 3D foundation for building a continuous magnetic rock property model of the basement unconformity surface. Mineral exploration targets in covered Paleozoic and Proterozoic terrains are associated with steeply dipping and variably magnetic formations with approximately 90% of the magnetic signal contributed directly by the unconformity surface (Pratt et al., 2019). An expert system AI methodology is used to build a geologically sensible, 3D magnetic formation and rock property model of the unconformity. Every magnetic anomaly on every line is modelled by a segment at the unconformity surface and assigned a location, width, depth, azimuth, magnetic susceptibility and magnetisation vector. The initial properties of the model segments are computed directly from the tensor data using formulae outlined in Pratt et al. (2019). Each segment is a 3D object defined by its x, y location, strike length (line spacing), width and elevation which collectively represent a 3D model of the unconformity surface along with a set of rock properties for integration with other exploration datasets. For brevity, we call it RPD Mapping for rock property and depth mapping.

The multistage process (Fig. 10) progressively refines the geological model using both geological principles and geophysical inversion of the magnetic tensor (Pratt & McKenzie, 2009). Importantly, the 3D geological model ensures that the computed compact magnetic properties are focused on the target unconformity and not subject to the dilution incurred by unconstrained voxel inversion methods that attempt to resolve the full geological volume (Foss & Austin, 2021). In this way we have the best chance of correctly matching the computed properties with the average magnetic properties for each formation. If shallow high susceptibility magnetic material is present in the cover rocks, then the RPD Mapper method will detect the shallow material rather than the target unconformity. This is not a problem in the study area.

In this study, we explore the benefits of RPD Mapping for greenfields exploration in the mature Mount Isa Inlier where there are many mineral deposits with regional geophysical and geological mapping coverage. RPD Mapping is suitable for exploration beneath cover because it automatically estimates a depth for each geological model segment.

Anomalous accumulations of magnetite along fault and fracture zones provide a targeting vector to possible associated mineral accumulations. The mineralisation could be coeval, nearby and/or associated with later alteration. Magnetic remanence could also indicate the presence of pyrrhotite which is a direct indicator of the presence of sulphides in the system. We test some of these ideas in the context of known deposits and look at the possibility for using the RPD Mapping method to highlight targets in an area that is well explored, but extremely complex.

GEOLOGY AND SURVEY DATA

Overview of the geology

The Mount Isa Inlier is among the world's most productive mineral provinces, containing Cu, Au, IOCG, Ag-Pb-Zn and U deposits (Williams, 1998). The Mount Isa Inlier was formed between ca. 1.9 and 1.5 Ga via a complex history, including three depositional phases and associated "cover sequences," four major magmatic events, and one major orogenic event. For a detailed discussion of the geology of the Eastern Succession, refer to Blenkinsop et al. (2008) and Foster and Austin (2008). The Isan Orogeny, which occurred from ca. 1.6 to 1.5 Ga, consisted of several stages of ductile through to brittle deformation, of which five are recognised in the Eastern Succession (Cloncurry Region; Austin and Blenkinsop, 2010).

Several workers (e.g., Butera, 2004; Mustard et al., 2004; Ford and Blenkinsop, 2008; Austin and Blenkinsop, 2009) have considered the prospectivity of a range of fault orientations in the Eastern Succession and have concluded that jogs, splays and intersections along north to north-northwest, northwest and west-northwest-trending faults provide the highest prospectivity for mineralisation of Cu and Au. From ca. 1510 Ma, crustal relaxation ensued in conjunction with the final and largest magmatic phase, intrusion of the Squirrel Hills Granite at ca. 1500 Ma. Breccias were overprinted by potassic ± chlorite alteration associated with brittle fault development in conjunction with east-southeast directed shortening and by subsequent reactivation associated with quartz-hematite alteration. Minor kinking and reactivation of pre-existing faults took place, facilitating some redistribution of Cu and Au within the mineral system, leading to the development of minor epithermal mineralisation and overprinting of pre-existing mineral deposits (Austin and Blenkinsop, 2009) e.g., Ernest Henry.

We used the 2018, 1:100,000 scale GIS mapping (Fig. 1) from the Geological Survey of Queensland (GSQ) as a major source of data for recognition of formation lithology, basic intrusions, granites, local structures and regional structures.

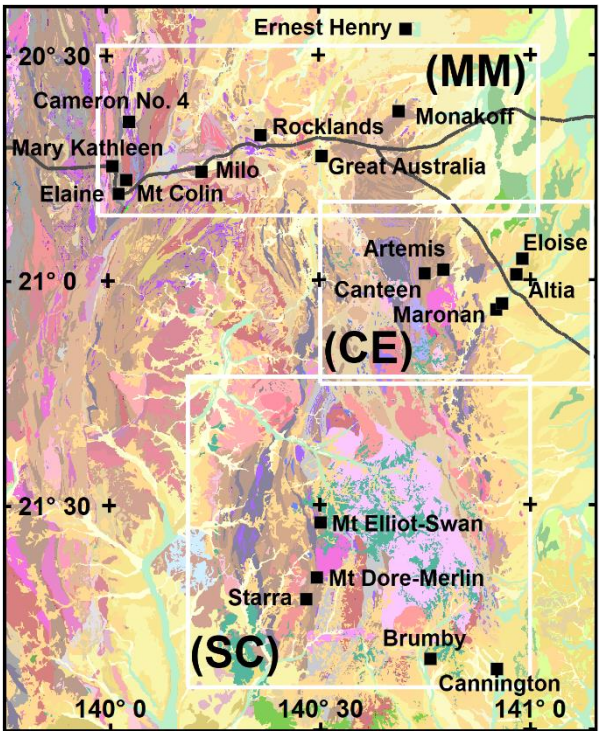

Figure 1. Map showing the 1:100,000 scale geological mapping of surface geology and sub-project areas (MM, CE, SC). Black squares show significant discoveries.

Historical geophysical data

We decided to use the aeromagnetic survey data available on the GSQ website that was acquired between 1990 and 1992. Most of the survey was flown by MIM (now Glencore), but also includes surveys flown by BHP, Ashton and Placer. The line spacing varies between 200 and 400 metres and was acquired east-west with north-south tie lines and a terrain clearance between 70 and 80 metres. In the absence of sensor elevation data, we used radar altimeter data in combination with an SRTM dataset from Geoscience Australia to provide an initial estimate for the sensor elevation and then applied a low pass filter to approximate the probable behaviour of the aircraft as it climbed over the terrain. The absolute elevation information is required for construction of a 3D geological model that is consistent with the terrain. A 50 metre resolution grid of the levelled total magnetic intensity data was also downloaded from the GSQ website and this grid provided the foundation for computation of the magnetic tensor grids (Pratt et al., 2020) which were then resampled at a 6 metre interval onto the original flight lines using a bicubic interpolator. The full dataset is large and we used a subset covering 64,000 line kilometres over three sub-areas as shown in Figure 2.

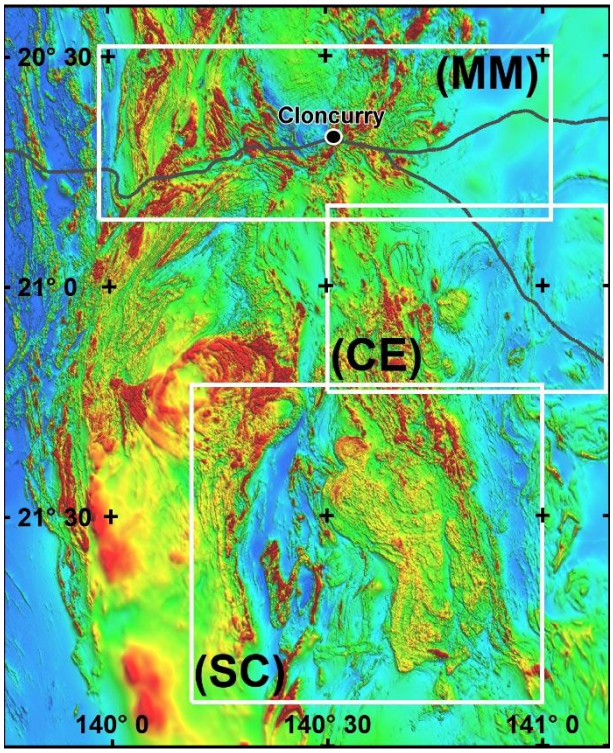

Figure 2. An image of the reduction to pole grid derived from the TMI grid supplied by the GSQ (Inclination -51.3 degrees, declination 6.5 degrees). The three sheets cover areas designated as (MM) Mount Colin to Monakoff, (CE) Canteen to Eloise and (SC) Starra to Cannington.

We used the historical data because it was acquired prior to the discovery and development of many of the deposits. After we started this project the GSQ released the data from the 2017 Cloncurry survey which was flown using a 100 metre flight line spacing. This high quality data will yield improved magnetic tensor estimates and provide new targets as well as improved results for existing targets.

RPD RESULTS

RPD processing of the three map sheets produced a model with a total of 86,942 3D segments, each with more than 160 attributes derived from the AI process and joint inversion of the tensor data. Many of the attributes relate to progressive refinement of spatial and magnetic properties along with geological shape parameters, connectivity and statistics. The main unconformity parameters that are useful in mapping and 3D applications include:

- Depth below ground
- Easting, northing and elevation
- Formation azimuth
- Susceptibility
- Resultant magnetisation
- Geological solid model (segments)
- Depth Quality.

We use the term "Depth Quality" to define an experimental parameter that is computed during the multi-stage AI procedure. Any information that can directly degrade the quality of the depth estimation is used to reduce the depth quality. Interference between adjacent anomalies has the largest impact and this is computed directly from the normalised source strength (Pratt et al., 2019). The Depth Quality parameter has a large impact on our ability to understand uncertainty in the results of the AI and inversion processes. We use this extensively to modify the size of attributed symbols when displaying magnetic susceptibility, magnetisation directions and depth. Larger symbols equate to higher confidence. A section of the Mount Colin to Monakoff (MM) sheet is used to illustrate different visualisation methods by layering the attribute data as point symbols over different image layers (Fig. 3).

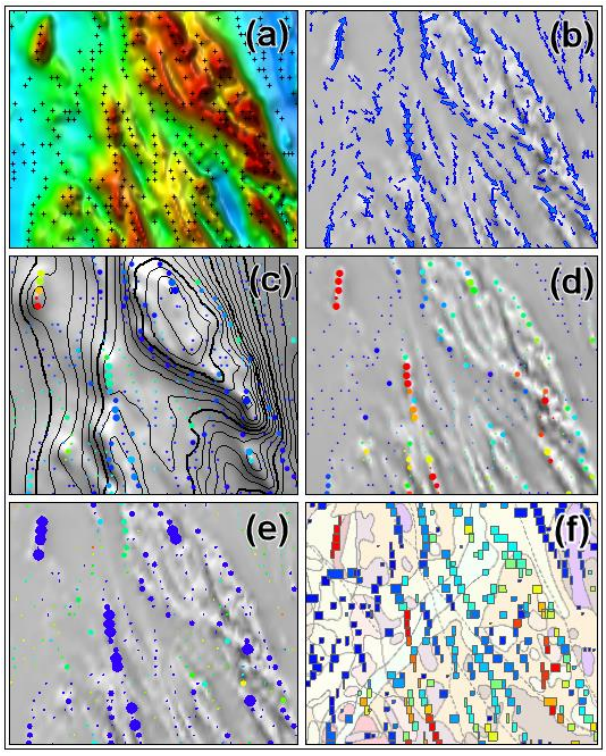

Figure 3. Rock property attributes displayed over different backdrops. (a) Segment centres over an RTP image, (b) formation azimuth symbol over a first vertical derivative (FVD image), (c) a colour coded symbol representing depth below ground with size coded by Depth Quality over a pseudo-gravity image, (d) colour coded magnetic susceptibility symbol with size encoded by Depth Quality over a FVD image, (e) colour coded apparent resultant rotation angled (ARRA) symbol size encoded by Depth Quality over a FVD image and (f) a segment model colour coded by magnetic susceptibility over the 1:100,000 geological outcrop map. Symbol colour tables use the standard blue-red with a linear stretch.

An example of a predominantly remanently magnetised unit is shown in Figure 4 where the resultant magnetisation vector declination is colour coded by the apparent resultant rotation angle (ARRA) and the direction is controlled by the resultant vector declination. The existence of remanence can also be seen clearly in the original magnetic image. The outline interpreted from the magnetic data matches the boundary of the Milo Beds where it outcrops. The unit continues north beneath cover and is bounded by a fault plane to the east. The metadata describes this unit as a metasiltstone, reversely magnetised and probably pyrrhotitic. A zinc mineral occurrence is located on the outcrop boundary.

The resultant magnetisation direction is an apparent direction which is only valid for compact magnetic sources (Clark, 2014, Pratt et al., 2014; Foss et al., 2019). Essentially this means that you can use it for many ore deposits and magnetic pipes. It can be used to calculate dip for normally magnetised linear magnetic anomalies or resultant magnetisation for vertical linear formations that are predominantly remanently magnetised. In the context of the Milo Beds it is not possible to recover the true magnetisation direction, but we can look for systematic changes in the vector direction that may provide an indication of changes in the magnetic rock properties. The change in declination at the southern end is possibly associated with a pre-folding, strong magnetic remanence direction.

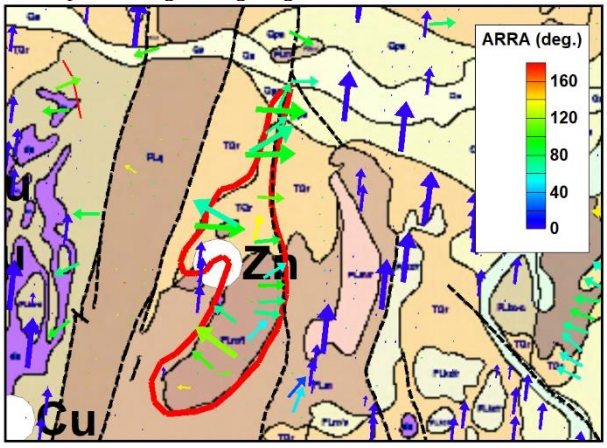

Figure 4. An example of a remanently magnetised formation with vectors showing the magnetisation direction and colour coded by ARRA. The red boundary, which was mapped from the magnetic data, is related to the metasiltstone Milo Beds, believed to contain pyrrhotite. Blue vectors represent the induced field magnetisation.

Cross-line magnetic trends depend on the gridding technique which impacts on the estimation of the cross-line tensor components. We are working on a separate research program to investigate new techniques for improving the 1990 Cloncurry across-line grid trend quality and estimation of the magnetic tensor.

TARGET GENERATION

In the Cloncurry region, a locally anomalous accumulation of magnetite or pyrrhotite is a potential vector to possible nearby mineralisation such as IOCG, skarn and Pb/Zn deposits. Target weighting factors relevant to this study include:

1. High magnetic susceptibility estimates provide a quantitative approach to the detection of high magnetite concentrations that account for changes in cover depth.

2. Detection of anomalous remanence has a possible pyrrhotite association which indicates the presence of sulphides. (Austin et al., 2013, 2017)
3. Nearby magnetite destruction is a positive indicator and may be associated with late-stage alteration that can carry mineralising fluids (Austin et al., 2013, 2017)
4. Nearby crustal scale structures and breccia zones are important conduits for mineralising fluids (Austin & Blenkinsop, (2009).
5. A local secondary structure improves the target significance, especially those that suggest dilation (Austin & Blenkinsop, (2009).
6. Nearby igneous intrusions that could drive fluids through local structures.
7. Host rock chemistry has potential for predicting the probable mineralisation style (i.e., IOCG, skarn, Pb/Zn).

Factors 1 to 6 are used to develop a RPD weighting parameter for ranking of identified targets. Importantly, all six parameters can be interpreted from the magnetic data even if geological mapping data is not available for areas under cover.

Local geological knowledge can further extend the weighting of targets by using parameters such as:

- Preferred local structural direction (where available)
- Local structure age
- Proximity to existing major deposits/prospects
- Local mineral occurrences
- Local geochemical anomalies
- Radiometric indicators related to transitional redox zones.

Using these principles, we manually identified 67 targets from magnetic image products that highlighted anomalous zones in the local geological context. Figure 5 shows two targets associated with a fault trend identified in the magnetic data overlain on a normalised source strength (Clark, 2014) colour image shaded by the first vertical derivative. We later discovered that both targets were present in the GSQ mineral occurrence database.

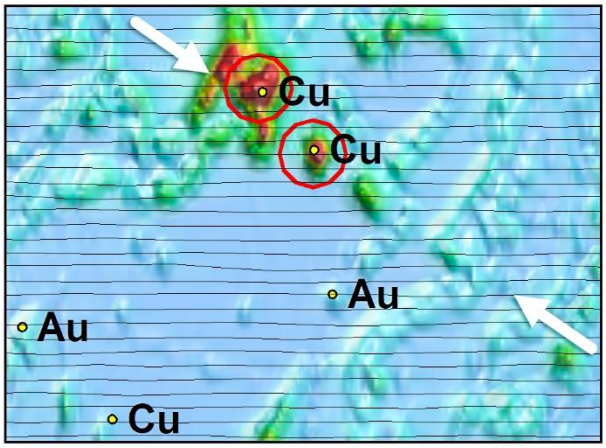

Figure 5. Example of two targets (red circles) selected by visual inspection of the magnetic imagery and identification of a possible northwest trending fault. Yellow dots show the location of mineral occurrence records along with the primary mineral from the GSQ database.

This manual study identified the Altia, Brumby, Canteen, Cannington, Eloise and Maronan discoveries. These discoveries are relatively easy to recognise by their magnetic anomaly amplitude, character and structural context. The RPD dataset provides an opportunity to apply more systematic procedures for interpreting the data and integrating geological information that is potentially coupled with deposit emplacement. The RPD point dataset was overlain on a selection of magnetic and geology map images to provide a context for assessment of each target. A total of 29 new targets were added to the unrated target set using the RPD data. Figure 6 shows an example display style for three RPD targets that occur along a mapped fault zone.

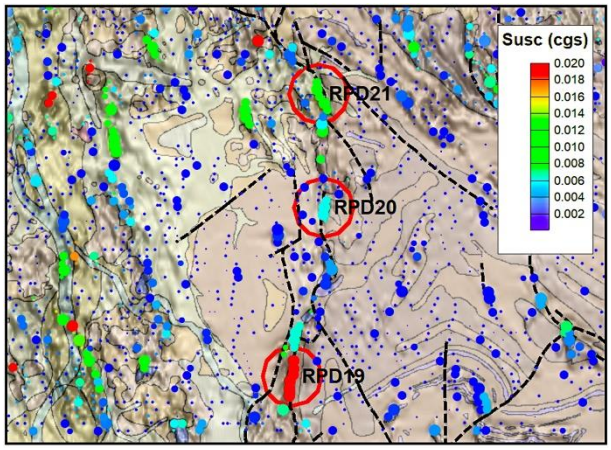

Figure 6. Manually selected RPD targets (red circles) highlight symbols coloured by magnetic susceptibility, superimposed on the 1:100,000 scale geology and structure mapping with a shadow of the first vertical derivative of RTP. Symbols are size encoded according to the AI Depth Quality assignment.

Apart from the obvious quantitative property information, the ability to layer point information over any other dataset without obscuring the underlying information improves our cognitive ability to see context sensitive correlations. It is easy to overlay the rock property symbols (RPDs) over blended images with other vector layers such as local and crustal scale structures.

We experimented with the six primary weighting factors for the 96 targets using the RPD properties magnetic susceptibility, possible evidence of magnetite destruction, remanence indicators, local and crustal scale structures plus nearby intrusions. The weights for the geological parameters were estimated from manual measurements of the shortest distance from the structures. The weights for nearby intrusions were assigned based on proximity and the scale of the intrusion.

We wanted to select the top 20 targets with an expectation that 50% could disappear upon closer inspection. Full magnetic modelling would be one of the tools designed to test the characteristics of the targets with close examination of shape, depth, susceptibility, magnetic remanence (Foss et al., 2019) and possible evidence for magnetite destruction (Austin et al. 2013, 2017).

COMPARISON WITH DISCOVERIES

We looked at the relationship between the six major discoveries with strong magnetic signatures and compared them against the interpreted weights. Cannington's estimated magnetic susceptibility is lower than the other discoveries and did not make the top 20 target list even with the inclusion of all the primary geological parameters. Other geological factors based on local knowledge and full modelling of the anomaly could change this outcome. The two magnetic anomalies associated

with Cannington stand out because they are located near a major northwest structure in a large zone that is magnetically quiet.

We found that five of the six targeted discoveries have susceptibility estimates of 0.5 SI (0.04 cgs) while the maximum for Cannington was estimated to be 0.125 SI. We used a boost for susceptibilities above the Cannington estimate to improve the separation of targets with higher magnetite concentrations (Fig. 7).

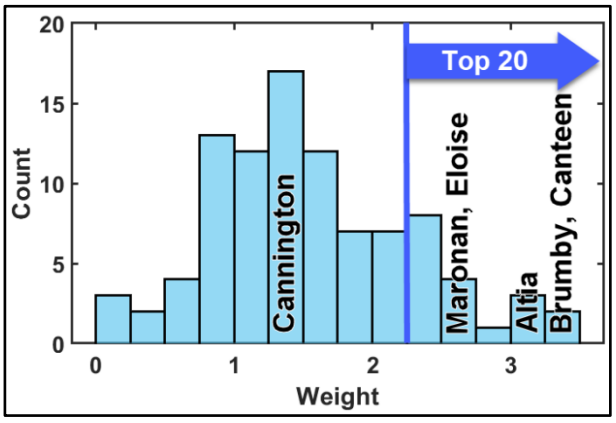

Figure 7. A histogram of the 96 target weights using a boost for susceptibilities over 0.125 SI (0.01 cgs). The six major discoveries detected in the targeting process are shown above their assigned weight bins.

For magnetic susceptibilities in the range of 0.125 - 0.5 SI units (0.01 - 0.04 cgs), the gross magnetite concentrations are estimated to range between 3% and 12%. The RPD target magnetic susceptibility estimates are expected to be lower than the average values for the rocks if the target dimensions are smaller than the inverted segment widths. The actual estimated values can be improved by detailed modelling and inversion where local geological constraints and demagnetisation computations can be applied (Foss et al., 2019).

Most of the targets identified in this study are in areas of outcrop or thin cover (<100 m) where there is more detailed information on structures and lithologies. Five of the six discoveries are beneath cover while the Canteen host rocks are exposed at the surface.

We used enhanced pseudo-gravity images (Pratt & Shi, 2004) to provide a visual understanding of the bulk magnetic properties of the local formations surrounding each of the targets. Figure 8(a) shows targets posted over an image of the pseudo-gravity for the SC sheet where the targets are colour coded by their computed total weight. The Brumby discovery appears with the highest weight in red along with two others that are not associated with discoveries but show close associations with local and crustal scale structures. The Cannington deposit is near the middle of the weight range and associated with a major structure. The SWAN discovery is believed to be associated with a magnetic breccia zone and is visible in the recent high resolution survey (Austin et al., 2021) but not detectable in the 1990 survey data.

Starra 222 and other nearby discoveries sit in hematite-rich zones to the east of a highly magnetic biotite-magnetite-pyrite schist. There are numerous structures along this trend, but the structure that hosts the deposits appears to be relatively late (Austin et al., 2021). The high-amplitude anomalies associated with the Starra trend were excluded from the target list because they appeared to be part of a magnetite-rich formation. That is where local knowledge of the geology becomes important for reassessment of the rock properties. Figure 8(b) shows the distribution of target magnetic susceptibilities using a histogram stretch for the symbol colour coding. The symbol colour distribution is similar to the distribution in Figure 8(a), but significant differences relate to the impact of the geological weights.

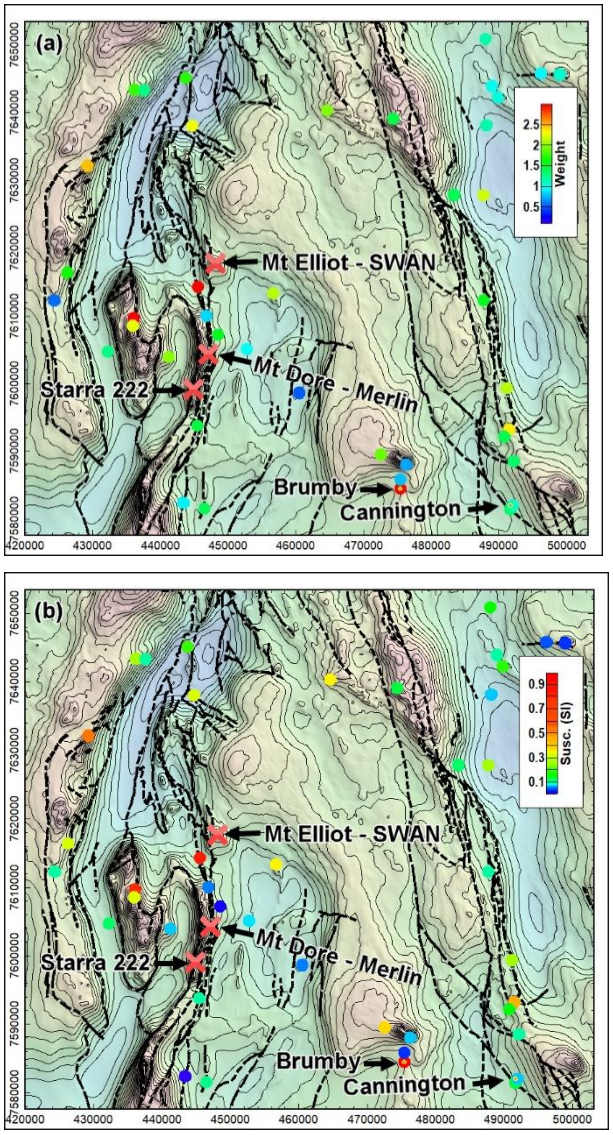

Figure 8. Map circular symbol distributions representing target weights (a) and target magnetic susceptibilities (b). A linear colour stretch is used for the target weight symbols and a histogram stretch is applied to the magnetic susceptibility symbols. The names of major discoveries are shown with arrows pointing to their locations. Undetected discoveries are shown with red crosses.

Figure 9 shows a plot of the estimated depths as colour coded symbols with depths in excess of 100 metres shown as orange to red colours. Blue is the dominant colour in areas of outcrop with mid-green indicating areas of transported cover, weathering or residual Jurassic sequence cover. Every segment in the underlying model is included in this image, but the symbol size is reduced to almost zero when the Depth Quality estimate falls below 50%. Rocks of Cambrian age cover the western margin of the SC sheet with depths increasing to the west and southwest. The shallow, east dipping Jurassic cover

of the Carpentaria Basin sequence appears along the eastern margin of the sheet.

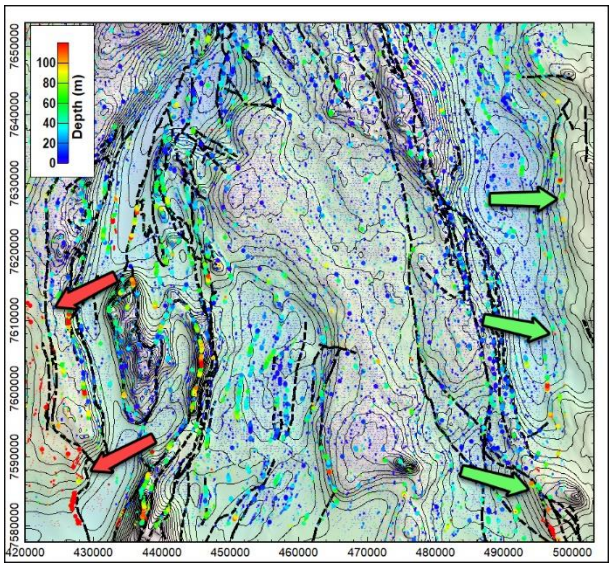

Figure 9. Estimated depth in metres below the ground surface displayed as colour modulated symbols and size encoded by the quality of the depth estimates. The red arrows show the location of Cambrian cover and green arrows show the location of Jurassic sedimentary cover.

CONCLUSIONS & RECOMMENDATIONS

The ranking approach combines both direct estimation of detailed magnetic properties with geological data that is relevant to the prediction of mineral occurrences. The magnetic inversion is performed at the detailed scale of individual flight lines, providing information suitable for both regional and local interpretation. When working locally, an experienced geologist can include additional relevant information such as preferred structural directions, preferred structure ages, host rock chemistry, density from detailed gravity surveys, surface geochemistry, radiometrics, EM and IP survey data. The high resolution magnetic property information, which includes magnetic susceptibility, depth, strike, width and possibly magnetic remanence indicators, can be used as inputs to AI systems to further enhance target rankings. AI systems such as weights of evidence (Austin and Blenkinsop, 2009), machine learning, self-organising maps (SOM) or random forests can utilise the additional information provided by parameters such as depth, Depth Quality and inversion statistics to enhance the focus on targets hosted close to the unconformity surface.

The rock property and depth mapping process provides high resolution estimates for the spatial and magnetic rock properties that is layered over image and GIS data as an attributed point set. While the property estimates are not as good as direct modelling of targets, it does provide a consistent, high resolution basis for assessment and reduces the need for interpretive modelling to only the highest ranked targets. The solid model can be used directly for further investigation of the target details through interactive constrained inversion. The data is easy to integrate with geophysical, GIS mapping or AI systems. The depth information can be used to map the basement unconformity or display the models and physical property estimates alongside drilling and other geophysical property models in 3D visualisation applications.

In this study we have focussed on the use of magnetic susceptibility to detect anomalous accumulations of magnetite as a vector to potential discoveries. This approach will not detect all potential targets, but it did detect six of the major discoveries in the study area and highlighted new targets. The detection of magnetite destruction and magnetic remanence provides an opportunity to improve the ranking of targets along with local geological knowledge, radiometric, mineral occurrence and geochemistry data. We used the available public domain magnetic grid, but the original data will need re-gridding to improve the quality of the tensor for the cross-line magnetic tensor components. Now that a new 100m line spacing dataset is available, we expect the RPD Mapping process will improve recognition of magnetite destruction/alteration and magnetic remanence.

ACKNOWLEDGEMENTS

We would like to acknowledge the constructive suggestions made by the anonymous reviewer which resulted in improved clarity and reorganisation of some content.

REFERENCES

Austin, J.R., and Blenkinsop, T.G., 2010, Cloncurry Fault Zone: Strain partitioning and reactivation in a crustal-scale deformation zone, Mt Isa Inlier: Australian Journal of Earth Sciences, 57, 1–21.

Austin, J.R., and Blenkinsop, T.G., 2009, Local to regional scale structural controls on mineralization and the importance of a major lineament in the eastern Mount Isa Inlier, Australia: Review and analysis with autocorrelation and weights of evidence: Ore Geology Reviews, 35, 298–316.

Austin, J.R., Clark, D.A., Schmidt, P., Hillan, D. and Foss, C.A., 2013 Magnetic anomalies to mines: Practical insights into the myths, methods and mysteries in relating mineralisation and magnetisation: Extended Abstract, 23rd International Geophysical Conference and Exhibition, 11-14 August 2013 - Melbourne, Australia, 6p.

Austin, J.R., Patterson, B., leGras, M., Burchall, R., Walshe, J., 2017, Geophysical Signatures of IOCG and Sedex style mineralization in the Mount Isa Eastern Succession, Queensland, Australia. Exploration 17: 6th Decennial International Conference on Mineral Exploration, Toronto, Canada, 16p.

Austin, J.R., Schlegel, T., Bjork, A. and Foss, C.A., 2021, Geophysical proxies for redox and pH gradients in IOCG systems: Cloncurry District, Qld, Australia; 3rd AEGC: Geosciences for Sustainable World – 15-20 September 2021, Brisbane, Australia.

Blenkinsop, T.G., Huddlestone-Holmes, C.R., Foster, D.R.W., Edmiston, M.A., Lepong, P., Mark, G., Austin, J.R., Murphy, F.C., Ford, A. and Rubenach, M.J., 2008, The crustal scale architecture of the Eastern Succession, Mount Isa: The influence of inversion: Precambrian Research, 163, 31–49.

Butera, K.M., 2004, The role of mafic rocks in the genesis of IOCG and base metal deposits, Mount Isa Eastern Succession, NW Queensland, Australia: in A. C.Barnicoat, and R.J. Korsch, eds., Predictive Mineral Discovery Cooperative Research Centre — June 2004 Conference, Geoscience Australia, Canberra, Geoscience Australia, 21–22.

Clark, D. A., 2014, Methods for determining remanent and total magnetization of magnetic sources – a review: Exploration Geophysics, 45, 271–304.

Ford, A., and Blenkinsop, T.G., 2008, Combining fractal analysis of mineral deposit clustering with weights of evidence to evaluate patterns of mineralization: Application to Cu deposits of the Mount Isa Inlier, NW Queensland, Australia: Ore Geology Reviews, 33, 435–450.

Foss, C.A. and Austin, J.R., 2021, Why we should not report unconstrained inversion output in densities or magnetic susceptibilities, Extended Abstracts, 3rd AEGC: Geosciences for a Sustainable World, Brisbane.

Foss, C.A., Heath, P., Wise, T. and Dutch, R., 2018, Combined gravity and magnetic studies of satellite bodies associated with the giant Coompana negative magnetic anomaly in South Australia: ASEG Extended Abstracts, 2018

Foster, D.R.W., and Austin, J.R., 2008, The 1800 to 1610Ma stratigraphic and magmatic history of the Eastern Succession, Mount Isa Inlier, and correlations with adjacent Paleoproterozoic terranes: Precambrian Research, 163, 7–30.

Mustard, R., Blenkinsop, T., McKeagney, C., Huddleston-Holmes, C. and Partington, G., 2004, New perspectives on IOCG deposits. Mt Isa Eastern Succession, northwest Queensland: 74th Annual International Meeting, SEG, Extended Abstracts, 281–284.

Pratt, D.A. and Shi, Z., 2004, An improved pseudo-gravity magnetic transform technique for investigation of deep magnetic source rocks: Extended Abstracts, ASEG 17th Geophysical Conference and Exhibition, Sydney 2004.

Pratt, D.A. and McKenzie, K.B., 2009, Maximising geological information recovery from different magnetic instruments through the application of joint inversion, ASEG Extended Abstracts, 2009:1, 1-13, DOI: 10.1071/ASEG2009ab047

Pratt, D.A., McKenzie, K.B. and White, A.S., 2014, Remote remanence estimation (RRE): Exploration Geophysics, 45(4), 314-323.

Pratt, D.A., McKenzie, K.B. and White, A.S., 2019, An AI approach to automated magnetic formation mapping beneath cover: Extended Abstracts AEGC 2019: From Data to Discovery – Perth, Australia. ASEG Extended Abstracts, 2019:1, 1-9

Pratt, D.A., White, A.S., Parfrey, K.L. and McKenzie, K.B., 2020. ModelVision User Guide, p. 561 – 565. Version 17.0, Tensor Research Pty Ltd.

Williams, P.J., 1998, Metalliferous economic geology of the Mt Isa Eastern Succession, Queensland: Australian Journal of Earth Sciences, 45, 329–341.

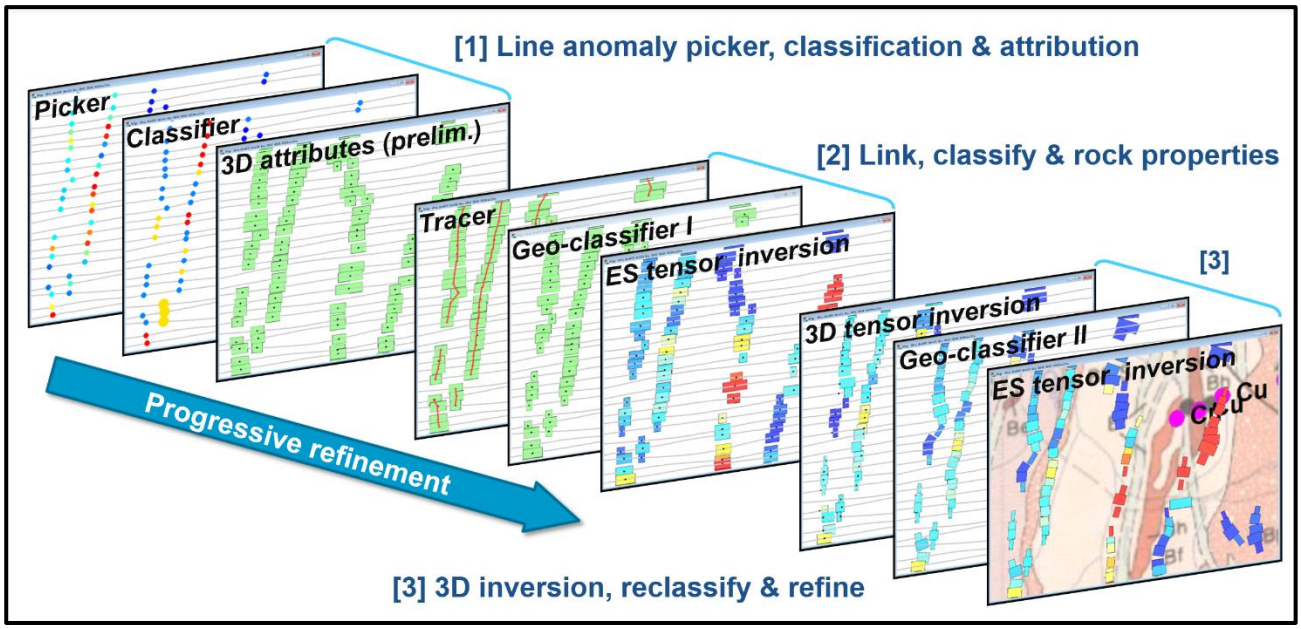

Figure 10. A diagrammatic representation of the sequential stages in the AI system used to convert full tensor magnetic data to a 3D model of the unconformity surface. Stage [1] produces a starting model that creates a 3D located segment and magnetic properties for every anomaly on every line. Stage [2] refines the model by connecting segments along geological trends and then runs an equivalent source inversion to improve the magnetisation estimates. Stage [3] runs a multi-segment inversion that adjusts segment position along the line, their thickness and magnetisation followed by an equivalent source inversion that re-inverts the magnetisations for changes made in the Geo-classifier II refinement step.